

## Probing the Gas-Phase Folding Kinetics of Peptide Ions by IR Activated DR-ECD

Cheng Lin,<sup>a</sup> Jason J. Cournoyer,<sup>a,b</sup> and Peter B. O'Connor<sup>a</sup>

<sup>a</sup> Mass Spectrometry Resource, Department of Biochemistry, Boston University School of Medicine, Boston, Massachusetts, USA

<sup>b</sup> Department of Chemistry, Boston University, Boston, Massachusetts, USA

The effect of infrared (IR) irradiation on the electron capture dissociation (ECD) fragmentation pattern of peptide ions was investigated. IR heating increases the internal energy of the precursor ion, which often amplifies secondary fragmentation, resulting in the formation of *w*-type ions as well as other secondary fragments. Improved sequence coverage was observed with IR irradiation before ECD, likely due to the increased conformational heterogeneity upon IR heating, rather than faster breakdown of the initially formed product ion complex, as IR heating after ECD did not have similar effect. Although the ECD fragment ion yield of peptide ions does not typically increase with IR heating, in double resonance (DR) ECD experiments, fragment ion yield may be reduced by fast resonant ejection of the charge reduced molecular species, and becomes dependent on the folding state of the precursor ion. In this work, the fragment ion yield was monitored as a function of the delay between IR irradiation and the DR-ECD event to study the gas-phase folding kinetics of the peptide ions. Furthermore, the degree of intracomplex hydrogen transfer of the ECD fragment ion pair was used to probe the folding state of the precursor ion. Both methods gave similar refolding time constants of  $\sim 1.5 \text{ s}^{-1}$ , revealing that gaseous peptide ions often refold in less than a second, much faster than their protein counterparts. It was also found from the IR-DR-ECD study that the intramolecular H<sup>+</sup> transfer rate can be an order of magnitude higher than that of the separation of the long-lived *c/z* product ion complexes, explaining the common observation of *c*- and *z* type ions in ECD experiments. (J Am Soc Mass Spectrom 2008, 19, 780–789) © 2008 American Society for Mass Spectrometry

One of the major challenges of modern structural biology is to understand the process of *in vivo* folding of a protein into a well-defined, biologically active structure [1, 2]. The effects of aqueous solvation and the intrinsic intramolecular interactions may be better revealed by studying the protein conformation in the gas phase in the absence of solvents. Making use of the soft ionization method of electrospray ionization (ESI) [3], a number of mass spectrometry (MS) based methods have been applied to investigate the protein conformation in the gas phase, including the ESI charge state distribution to determine the availability of ionization basic sites [4, 5], H/D exchange (HDX) to identify the exposed region of the conformation [6–10], drift tube ion mobility spectrometry (IMS) to measure the conformational cross section [10–13], high-field asymmetric waveform ion mobility spectrometry (FAIMS) to separate different conformers [10, 14, 15], infrared photodissociation spectroscopy (IRPDS) to probe the hydrogen bonding [16–20], and electron capture dissociation (ECD) [21, 22] to locate the

noncovalent tertiary bonding [23–26]. Particularly, ECD based methods have been used to study the gas-phase unfolding and refolding kinetics of protein ions [24, 25].

ECD in Fourier-transform ion cyclotron resonance mass spectrometry (FT-ICR-MS or FTMS) [27, 28] has quickly found wide application in both top-down and bottom-up proteomics [21, 29–33], as well as in identifying and locating post-translational modifications (PTMs) [34–38]. As a nonthreshold dissociation method, the ECD fragment ion yield of a protein ion is not only affected by its sequence, but also by its higher order structures [15, 21, 26, 39, 40]. This is the basis of studying protein conformation and folding process by ECD. Noncovalent intramolecular interactions of protein ions may prevent fragment ion separation, leading to decreased product ion yield and poor sequence coverage, both of which can be improved in activated ion (AI)-ECD, where protein ions are unfolded [41–45]. Ion activation is typically done by collisions with background gas molecules [41, 43, 45], raising the ambient temperature [16, 45], or infrared (IR) laser irradiation [42, 44–46]. Efficient energy-transfer via multiple collisions with gas molecules requires the cell pressure to be increased to the  $10^{-6}$  torr range, which in turn requires a long pump-down time ( $\sim 10 \text{ s}$  typically) before the

Address reprint requests to Dr. Peter O'Connor, Department of Biochemistry, Boston University School of Medicine, Boston, MA 02118, USA. E-mail: poconnor@bu.edu

pressure is suitable for trapped ion excitation and detection with a sufficiently long transient for good resolving power, making it unattractive for high-throughput analysis or signal averaging when the sample comes in limited amount. Moreover, collisional activation via sustained off-resonance irradiation (SORI) [47, 48] of precursor ions is complicated by tuning of optimal conditions for each individual ion, while “in-beam” activation (as in in-beam ECD [41] or plasma ECD experiments [43]) has the limitation of not being able to isolate the precursor ions. Raising the temperature to and keeping it at a well defined value in the ICR cell is not always possible with every FT-ICR mass spectrometer [49, 50]. Even when it is possible, it is still inconvenient in that it takes time to heat up the cell before AI-ECD experiments and to cool the cell back down for normal operation afterwards. Furthermore, heating also usually results in an undesirable increase in cell pressure. IR irradiation, on the other hand, is fast, easy to implement, allows precursor ion isolation, and does not result in a cell pressure increase, making it the preferred method for ion activation in AI-ECD experiments.

Simultaneous introduction of the IR laser and electron beam to intersect the ion cloud in the center of the ICR cell has been previously done by either bringing in one beam off-axis while keeping the other on-axis [42, 45], or introducing the IR beam through a hollow electron gun mounted on-axis and letting the ring-shaped electron beam be compressed by the magnetic field gradient [44]. It has been shown extensively that ion activation by IR laser absorption leads to enhanced fragmentation in protein ion ECD. The heated, unfolded protein ion can also cool and refold in the gas phase, and ECD fragment ion yield with ECD conducted at various delays after the IR irradiation should provide a measure of the extent of protein refolding [25].

It should be noted that the increased product ion formation results from the breakdown of the initially formed long-lived fragment ion complexes that stay unseparated during the excitation/detection event in the absence of ion activation. Unlike larger protein ions, intramolecular noncovalent interactions in peptide ions are not as numerous. Thus, the resulting fragment ion complexes in ECD are often short-lived, and easily separate to generate individual product ions before ion detection. Consequently, little enhancement in fragment ion yields were expected in AI-ECD of smaller peptide ions. Nonetheless, the existence of these ion complexes in peptide ECD is evident, as suggested by a number of experiments. Deuterium scrambling in ECD of a selectively deuterated linear peptide was readily present, most likely due to intermolecular H/D exchange in the fragment ion complexes [51]. Formation of radical  $c$ -ions and even-electron  $z$  ions is often observed in peptide ECD experiments, postulated to be the result of H-atom abstraction from the  $c$ -ion backbone or side chains by the  $\alpha$ -carbon radical on the  $z$ -ion [51–53]. This hypothesis correlates well with the observation

of the decreased  $c\cdot/c$  ratio and the increased  $z\cdot/z$  ratio upon ion activation [53], when  $c/z$  ion separation rate is comparable to that of the H-atom transfer. The knowledge that the  $c\cdot/c$  ratio decreases and the  $z\cdot/z$  ratio increases upon ion activation has been utilized to distinguish the type of ions formed in ECD [53]. Finally, in double resonance (DR)-ECD experiments, resonant ejection of the charge reduced species and the isobaric fragment ion complexes resulted in abundance decreases of many ECD fragments from peptide ions, thus directly showing that formation of these ECD fragment ions proceeds via radical complex intermediates that have a lifetime at least comparable to that of the ejection time, typically in milliseconds [54].

## Experimental

Experiments were carried out on a custom-built qQq-FT-ICR mass spectrometer with an external electrospray ionization source [55, 56]. All peptides were purchased from Sigma Aldrich (St. Louis, MO), and used without further purification. The samples were diluted to  $\sim 5$  pmol/ $\mu$ L in 49.5:49.5:1 H<sub>2</sub>O:CH<sub>3</sub>OH:HCOOH solution, and electrosprayed from glass capillary nanospray tips to generate multiply charged ions. Ions of interest were isolated and accumulated in the front end quadrupoles before entering the cell, where they were subjected to  $\sim 100$  ms low-energy electron irradiation from an on-axis indirectly heated dispenser cathode (model STD200; Heatwave, Watsonville, CA). In double resonance experiments, the charge reduced molecular ions were resonantly ejected from the cell by applying a single frequency excitation waveform with peak-to-peak amplitude of 2.5 to 40 V during the electron irradiation period.

IR light (10.6  $\mu$ m) from a CO<sub>2</sub> laser (Synrad, Mukilteo, WA) was introduced into the ICR cell through a BaF<sub>2</sub> window,  $\sim 0.87$  in. off center. The IR laser beam traveled parallel to the magnetic field axis towards a mirror mounted on the cell end trapping plate, with the mirror tilted at  $\sim 4.2^\circ$ , such that the reflected beam passed through the center of the cell. For initial alignment, a photodiode was installed on the other cell trapping plate, located diagonally from the mirror, also  $\sim 0.87$  in. off center. Overlap of the reflected beam from an alignment diode laser (590 nm) mounted just outside of the laser exit and the photodiode was optimized by maximizing the photoconductivity of the photodiode. The laser beam path was then constructed and defined by insertion and locking of two irises around the beam, and the photodiode was removed as it was not UHV compatible. Final alignment was achieved by maximizing the fragmentation of ubiquitin ions by the 10.6  $\mu$ m laser. With the IR beam intersecting the ion cloud at an angle, higher fragmentation yield may be achieved by increasing the trapping voltage to squeeze the ion cloud axially. However, such was not implemented in

IR-DR-ECD experiments, as the objective was merely to heat up the ions gently rather than to achieve maximum fragmentation. The IR irradiation time was adjusted to achieve maximum ion activation without fragmentation.

A typical spectrum was the sum of 10 scans, acquired at 1 MHz sampling rate and with 512 k point buffer size, corresponding to a 0.524 s transient. The digitized transients were zero-filled twice and fast Fourier transformed without apodization to produce the magnitude mode mass spectra. Because all fragment ions were singly charged, their abundances were calculated directly from peak heights without the need of charge correction to account for ICR response. With the theoretical Fourier-transform limit mass resolving power ( $f^2t/2$ ) being a mere 28,134 at  $m/z \sim 1000$ , it was not possible to separate the  $A + 1$  isotopic peak of  $c$ - or  $z$ -ions from the monoisotopic peak of the corresponding  $c$  or  $z$  ions. Thus, when interference existed, the theoretical  $A + 1$  contribution from the odd-electron species was subtracted to give the correct ion abundance of the monoisotopic even-electron species.

## Results and Discussion

### Effects of IR Heating on ECD Pattern of Substance P

As a first example to show the effects of IR heating on ECD pattern of peptide ions, the ECD spectra of Substance P (RPKPKQFFGLM-NH<sub>2</sub>) both without (Figure 1a) and with IR heating (200 ms duration) before (Figure 1b) and after (Figure 1c) electron irradiation were acquired. Since both basic residues are located near the N-terminus, it is of no surprise that ECD of Substance P produced mostly  $c$  type ions, with the only  $z$  type ion being the  $z_9$  that contains the lysine residue. The  $c_2$  ion is not present in the spectrum, even though its  $m/z$  (273.2) is well above

the Nyquist frequency limit used (corresponding to  $m/z \sim 215$ ). Post-heating the ion cloud with 200 ms IR irradiation did not change the ECD pattern significantly, with the  $c_2$  ion still missing from the spectrum (Figure 1c). Therefore, the absence of  $c_2$  cannot solely be the result of intracomplex noncovalent bonding holding the fragment ion pair together. It has been reported that at 86 K, ECD of Substance P generated only two  $c$  ions ( $c_7$  and  $c_{10}$ ), which was proposed to be the result of reduced conformational heterogeneity at lower temperature [57]. The calculated low-energy gas-phase structures of doubly charged Substance P involve solvation of the protonated Lys3 away from the N-terminus [58]; thus, even at room temperature, the formation of  $c_2$  is disfavored. The addition of a third charge by either adding a proton or replacing a proton with a divalent metal ion significantly changed the gas-phase conformation of Substance P, particularly the solvation of the Lys3 proton, as evidenced by the abundant  $c_2$  ion formation [59]. In accordance with these results, preheating the precursor ions with IR also led to the formation of  $c_2$  (Figure 1b), likely due to the increased internal energy of the precursor ions by IR heating allowing the protonated Lys3 to be solvated near the N-terminus. The conformational change also led to the disappearance of the  $z_9$  ion, as  $c_2$  formation requires the protonated Lys3 side chain to be hydrogen bonded to the Pro2 carbonyl and neutralized during electron capture, preventing the Arg1 side chain from binding there, which was necessary for  $z_9$  formation. The disappearance of  $z_9$  ions with IR heating may also be the result of secondary fragmentation, although this is unlikely because neither smaller  $z_n$  ions nor internal fragment ions were observed. Since the conformational change had to take place before ECD to direct the formation of product ions/neutrals, post-heating the ions would not have similar effects.

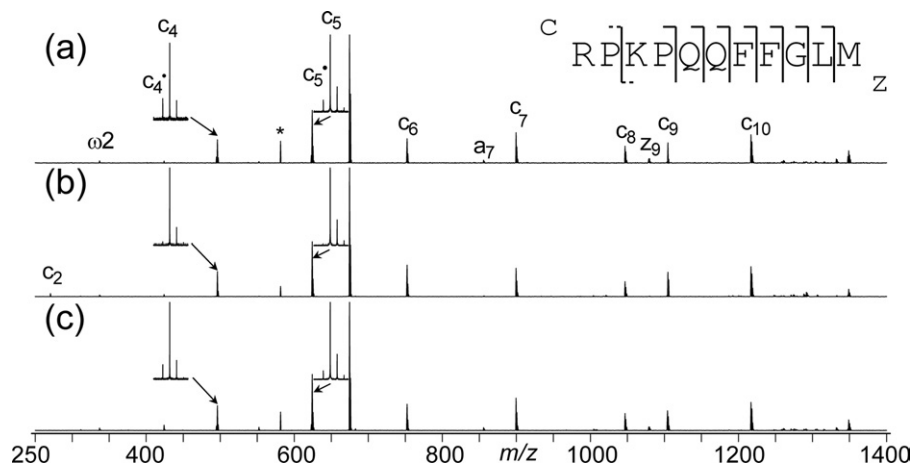


**Figure 1.** ECD spectra of Substance P with 150 ms electron irradiation and (a) no IR irradiation; (b) 200 ms IR irradiation immediately before the ECD event; and (c) 200 ms IR irradiation immediately after the ECD event. Asterisk marks electronic noise.

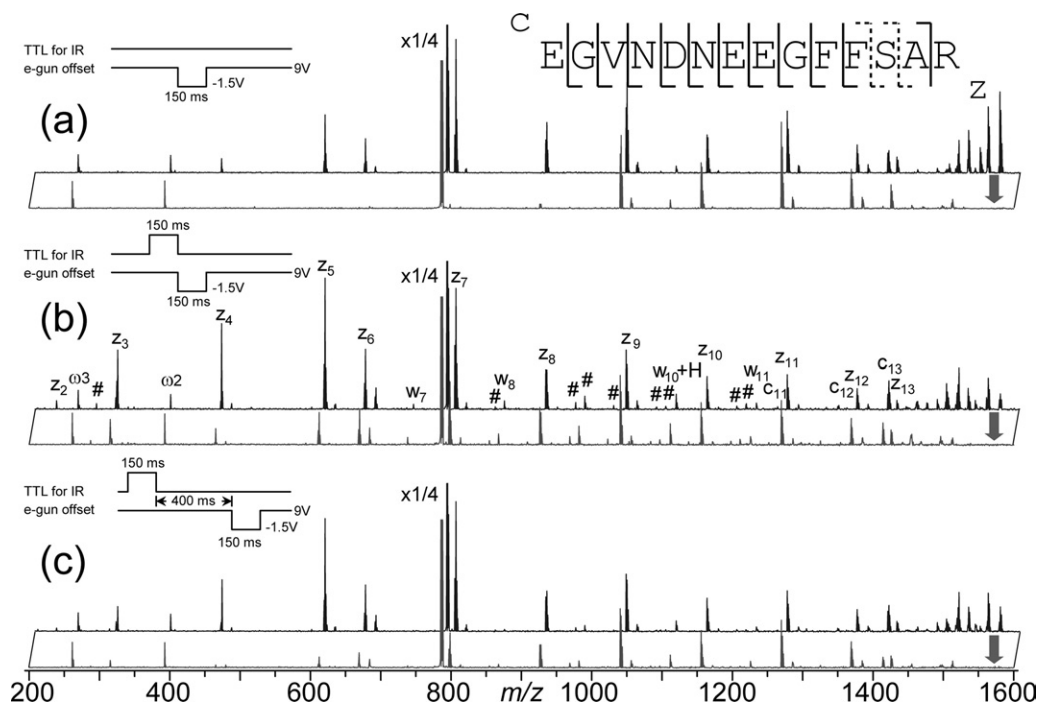


**Figure 2.** ECD (upper) and DR-ECD (lower) spectra of fibrinopeptide B with 150 ms electron irradiation and (a) no IR irradiation; (b) 150 ms IR irradiation immediately before the ECD event; and (c) 150 ms IR irradiation, followed by a 400 ms delay, before the ECD event. Insets illustrate the pulse sequence used in each experiment. For clarity, only *c*, *z*, and *w*-type ions are labeled, and the number symbol indicates secondary fragments corresponding to additional side-chain losses from *z*-type ions. Dashed cleavages are observed in AI-ECD only.

In addition to the commonly formed *c* and *z*-type ions, ECD of Substance P also produced some *c*-type ions ( $c_4$  and  $c_5$  as shown in the insets of Figure 1), which disappeared completely when the precursor ions were heated with IR irradiation before ECD. It is generally believed that ECD produces *c* and *z*-type ions first and the formation of *c*- and *z* ions is the result of intracomplex hydrogen radical transfer, the extent of which depends on the stability of the *z*-radical as well as the lifetime of the initially formed *c/z*-ion pair [51, 52, 54]. IR heating before ECD can disrupt the intramolecular interactions that hold the *c/z*-ion pair together, leading to shortened lifetime and less *c*- and *z* ion formation. On the other hand, post-ECD IR heating appeared to have very little effect, presumably because the intramolecular H transfer is a fast process that completed before the ion pair complex was heated sufficiently for dissociation. It is also interesting to note that  $c_4$  and  $c_5$  were the only two N-terminal fragment ions showing a significant drop in ion abundances in the DR-ECD experiment (Supplemental Figure 1, which can be found in the electronic version of this article), further suggesting that *c*-ion formation requires a long-lived ion pair complex. Although the abundances of  $c_4$  and  $c_5$  dropped significantly in DR-ECD, a substantial amount of *c*-ions remained. Thus, the intracomplex hydrogen radical transfer must have taken place on a

timescale at least comparable to that of ion ejection, i.e., in sub-ms.

#### Enhanced Fragment Ion Yield in IR-ECD

While fragment ion yield enhancement and improved sequence coverage in AI-ECD of protein ions were largely attributed to the breaking of noncovalent interactions to facilitate the fragment ion separation and detection, it is clear from the previous example that increased conformational heterogeneity may also play an important role. In IR-ECD of Substance P, this resulted in  $c_2$  ion formation and  $z_9$  disappearance with no other significant change in the ECD pattern. A more drastic change in the ECD pattern with IR heating was observed in IR-ECD of fibrinopeptide B (EGVNDNEEGFFSAR), as shown in Figure 2. ECD of fibrinopeptide B generates mostly *z* type ions due to charge retention on the C-terminal arginine side chain upon electron capture, with a small peak corresponding to the  $c_{13}$  ion (upper spectrum, Figure 2a).  $z_2$  ( $m/z \sim 230$ ) was missing from the spectrum, and  $z_3$  was barely observable. 150 ms IR irradiation before ECD (upper spectrum, Figure 2b) led to formation of the  $z_2$  ion, and a large abundance increase for many small *z* ions ( $z_3$  to  $z_6$ ) as well as  $c_{11}$  and  $c_{13}$  ions. In the DR-ECD experiment, *z*-ions up to  $z_8$  showed appreciable abundance drop upon resonant ejection of the charge reduced molecular ion (at  $m/z \sim 1571$ )

during the ECD event (upper spectrum, Figure 2a), suggesting that the C-terminal arginine side-chain was hydrogen bonded to the side chains of Asn4 to Glu8 at room-temperature, which is highly likely since this sequence contains three acidic residues. The folded structure may also sterically restrict the access of the N-terminal  $-\text{NH}_3^+$  group (or other charge sites) to the carbonyls of Gly9 through Ala13, thus minimizing ECD near this region. Such steric restriction would be removed and the conformation heterogeneity increased when the peptide was unfolded by IR heating before electron irradiation, resulting in the fragment ion yield increase as observed. To open up new fragmentation channels, the unfolding and the conformational change have to take place before the dissociation event. IR irradiation after ECD did not change the ECD pattern significantly (spectrum not shown). Once again, it shows that the increased fragment ion yield in AI-ECD of small peptide ions is more likely to be the result of conformational change than the ease of fragment ion separation.

### Secondary Fragment Ion Formation in IR-ECD of Fibrinopeptide B

ECD of a multiply charged peptide ion produces an even-electron fragment (*c* ion) and an odd-electron fragment (*z* ion). The radical site on the odd-electron fragment can initiate further reactions such as intracomplex hydrogen radical transfer which leads to the formation of *c*- and *z* ions [52], or secondary fragmentation with little or no activation barrier [22, 60–63]. Secondary side-chain fragmentation leading to the formation of *d*- and *w*-type ions is well documented in the ECD literature, and has found application in de novo sequencing for its ability to distinguish between Leu and Ile residues [44, 60, 64, 65]. Abundant *w* ion formation was apparent in the IR-ECD experiment (Figure 2b), in accord with previous observations in hot ECD and AI-ECD, where extra energy seemed to enhance the *w* ion formation. Many other secondary fragment ions (peaks marked with the number symbol in Figure 2b) were also present in the IR-ECD spectrum, corresponding mostly to side-chain losses from the *z* ions. It is important to heat up the precursor ion before ECD, instead of the fragment ions after ECD, as post-ECD IR irradiation generates little secondary fragment ions. This might be due to rapid radical stabilization [66–68] via radical rearrangement, such as intracomplex H transfer, proline ring opening, or radical trapping near the aromatic group, before IR heating. Secondary backbone fragmentations dominated the ECD spectra of cyclic peptides [22], but no internal fragment ions were found in the IR-ECD spectrum of fibrinopeptide B, presumably because of the charge locations at the termini.

### Unfolding and Refolding of Peptide Ions by IR Irradiation

AI-ECD has been used to study protein folding in the gas-phase, by monitoring the fragment ion yield, which often increases with ion activation, due to breaking of intramolecular hydrogen bonds that prevent fragment ion separation [24, 25]. The challenge of extending this method to peptide folding studies is that the lifetime of the fragment ion complexes from peptide ion ECD is often much shorter than the delay between the ECD event and ion excitation/detection, and as the result, nearly all fragment ions are readily detected, with or without ion activation. This difficulty may be circumvented by applying the DR-ECD method, where resonant ejection of the fragment ion complexes during ECD can reduce the fragment ion abundance [54]. Because of the rapid ejection time, even fragment ions from intermediates of millisecond lifetime, as is typical in peptide ion ECD, can experience significant abundance drop in DR-ECD, and the subsequent increase when IR irradiation is applied to unfold the precursor ions.

A greater abundance drop in DR-ECD indicates a longer lifetime of the intermediate through which the product ions are formed, as the result of a more folded structure of the precursor ion. Compared to the sharp abundance drop in DR-ECD of room-temperature fibrinopeptide B (upper spectrum, Figure 2a), many small *z* ions experienced only moderate to little drop in abundance with pre-ECD IR irradiation (lower spectrum, Figure 2b), suggesting that most of the intramolecular hydrogen bonds were already broken. The lifetime of the intermediate can be calculated by assuming that separation of a fragment ion pair follows first-order unimolecular dissociation kinetics [54]. Figure 3 plots the abundance of

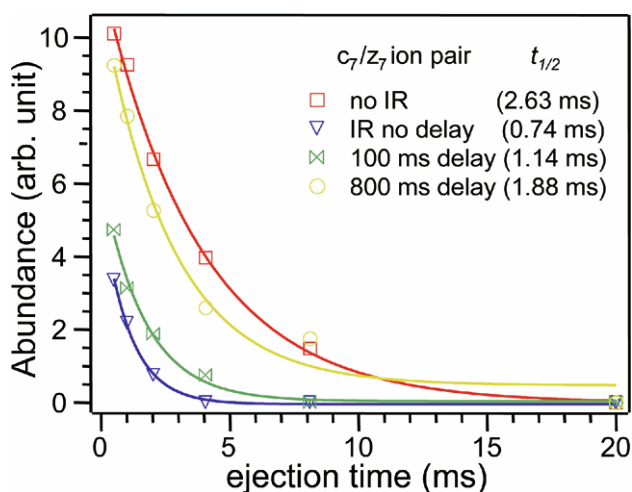


**Figure 3.** First-order decays of the intact  $c_7/z_7$  ion pair abundance as a function of ejection time when ECD of fibrinopeptide B was carried out at various delays after the IR irradiation. Solid lines are single exponential fits.

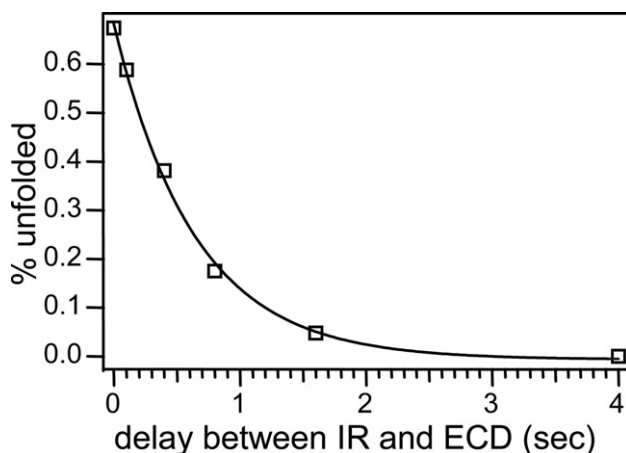


**Figure 4.** Percentage of the fibrinopeptide B ions that remained unfolded (as calculated from the DR-ECD experiment) at various time delays after the IR irradiation was turned off. Solid line is the single exponential fit.

the intact  $c_7/z_7$  pair, which is calculated as the difference between the abundance of  $z_7$  ion in normal ECD and that in DR-ECD, against the ejection time with DR-ECD taking place at various time delays after the IR irradiation (or without IR irradiation). The single exponential decay fit gives the lifetime of the  $c_7/z_7$  ion pair complex of  $\sim 2.6$  ms without pre-ECD IR heating, and  $\sim 0.7$  ms when ECD was performed immediately after the IR irradiation. When there was a delay between the IR and the DR-ECD event (Figure 2c), the lifetime of the intermediate increased to  $\sim 1.1$  ms with a 100 ms delay, and  $\sim 1.9$  ms with an 800 ms delay. Clearly, the unfolded peptide ion can cool and refold back to a more compact structure, particularly in absence of solvent molecules in the gas-phase. The refolding process took place in several hundred milliseconds to a few seconds, but a more quantitative assessment of the refolding time constant would require a properly constructed kinetic model.

#### Refolding Kinetics of Fibrinopeptide B Probed by the Fragment Ion Yield in DR-ECD

A simple two-state model was used to study the refolding kinetics, which assumes that a peptide ion can only exist in one of the two states: a folded state or an unfolded state. All  $c/z$  ion pairs from an unfolded peptide ion will break before ejection, but only a fraction ( $x$ ) of these ion complexes from a folded peptide ion will break before ejection. The value of  $x$  depends on both the amplitude of the resonant ejection waveform and the lifetime of the intermediate, and it can be obtained from the DR-ECD experiment without IR heating, assuming that all peptide ions are folded to start with. If DR-ECD is performed at a delay of  $t$  after the IR irradiation, then the ratio ( $r$ ) of the fragment ion abundance with resonant ejection to the one without resonant ejection can be expressed as:

$$r = y + (1 - y) * x \quad (1)$$

where  $y$  is the fraction of the peptide ions remaining unfolded at time delay  $t$ . This ratio ( $r$ ) should drop as the delay  $t$  increases and the peptide ions refold. Since  $r$  can be obtained experimentally, and  $x$  is just  $r$  without IR irradiation, the fraction of the unfolded peptide ions,  $y$ , at any given delay after the IR irradiation can be calculated according to eq 1. Assuming first-order refolding kinetics, one can obtain the refolding time constant  $k_{refold}$  by fitting  $y$  as a function of  $t$  to a single exponential decay. Figure 4 shows one such plot using the  $z_7$  yield in DR-ECD with 20 V<sub>pp</sub> ejection voltage as the probe for precursor ion folding state. Abundances from both the odd and even electron  $z_7$  ions are included, because the formation of either results from the breaking of the same initially formed  $c_7/z_7$  complex. The best fit gives a  $k_{refold}$  of  $1.55 \pm 0.10$  s<sup>-1</sup>, corresponding to a half-life of 0.45 s, which correlates well with Figure 2c. This is much faster than that for protein ions, which typically take minutes to refold in the gas phase [24]. Presumably, the reduced dimension of the potential energy surface of the smaller peptide ion makes it faster to find its low-energy structures than its protein counterparts.

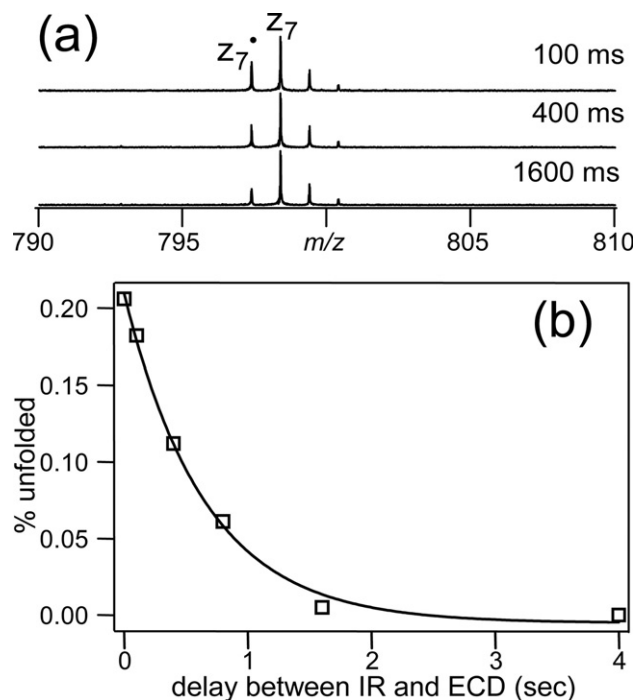


**Figure 5.** (a) Expanded regions of the ECD spectra of fibrinopeptide B showing that the percentage of the hydrogen transfer product ( $z_7$ ) increased as the delay between the IR and ECD events increased. (b) Percentage of the fibrinopeptide B ions that remained unfolded (as calculated from the ratio of  $z_7$  and  $z_7$  abundances) at various time delays after the IR irradiation was turned off. Solid line is the single exponential fit.

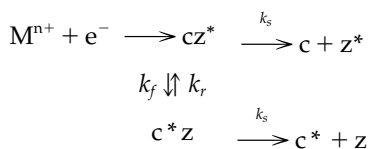
### Refolding Kinetics of Fibrinopeptide B Probed by the Intra-Complex Hydrogen Transfer

The key to the study of gas-phase peptide folding by AI-ECD is to find a suitable property that varies with folding states, such as the fragment ion yield in DR-ECD experiment (vide infra). Figure 5a shows that even though the total abundance of the  $z_7$  ions in ECD did not change much with the IR heating, the ratio of  $z$  to  $z\cdot$  ion abundance increased as the delay between IR and ECD increased. This should come as no surprise, as even-electron  $z$  ions are the products of intracomplex hydrogen radical transfer, which should decrease as the IR heating unfolds the peptide, leaving the product ion complex too short-lived to complete the H $\cdot$  transfer. The same two-state model can be used to study the peptide ion refolding, with a slightly different definition for folding and unfolding states. An unfolded peptide should only produce  $z\cdot$  ions, as there is nothing to hold the fragment ion pair together for H $\cdot$  transfer to take place. If a peptide is folded, however, a fraction ( $x$ ) of the  $z\cdot$  ions can abstract a hydrogen atom to form  $z$  ions, and the value of  $x$  can be obtained from the ECD experiment without IR heating, assuming all peptide ions are folded before IR irradiation. If  $y$  is the fraction of peptide ions remaining unfolded at a delay of  $t$  after IR, we have:

$$\frac{[z]_t}{[z]_t + [z^*]_t} = (1 - y) * x \quad (2)$$

Since the fraction of the even-electron  $z$  ions in the total  $z$  ion population can be directly measured in the ECD spectrum,  $y$  can be calculated for any given delay  $t$ . Once again, plotting  $y$  as a function of  $t$  should give a single exponential decay if the refolding process follows first-order kinetics. Figure 5b plots the percentage of the unfolded peptide ions against delay  $t$ , using the  $[z_7]/([z_7] + [z_7^*])$  to calculate  $y$ . The best fit gives  $k_{\text{refold}}$  of  $1.52 \pm 0.14 \text{ s}^{-1}$ , corresponding to a 0.45 s refolding time, nearly the same as that obtained in the IR-DR-ECD approach.

Furthermore, it is also possible to estimate the intracomplex H-transfer rate based on the abundance ratio of the even and odd-electron fragment ions and the fragment ion pair separation rate measured in the DR-ECD experiments. Scheme 1 illustrates the formation of  $c\cdot$  and  $z$  ions as the result of intracomplex H-transfer:



The rate equations for relevant species in scheme 1 are shown in eq 3:

$$\begin{aligned} \frac{d[cz^*]}{dt} &= -k_s [cz^*] - k_f [cz^*] + k_r [c^*z] \\ \frac{d[c^*z]}{dt} &= -k_s [c^*z] - k_f [c^*z] + k_r [cz^*] \\ \frac{d[z^*]}{dt} &= -k_s [z^*] \\ \frac{d[z]}{dt} &= -k_s [c^*z] \end{aligned} \quad (3)$$

Equation set 3 can be solved analytically, giving:

$$\begin{aligned} [cz^*]_t &= \frac{[cz^*]_0}{k_f + k_r} [k_r e^{-k_s t} + k_f e^{-(k_f + k_r + k_s)t}] \\ [c^*z]_t &= \frac{[cz^*]_0}{k_f + k_r} [k_f e^{-k_s t} - k_f e^{-(k_f + k_r + k_s)t}] \\ [z^*]_t &= \frac{[cz^*]_0}{k_f + k_r} \left\{ k_r [1 - e^{-k_s t}] + \frac{k_s k_f}{k_f + k_r + k_s} [1 - e^{-(k_f + k_r + k_s)t}] \right\} \\ [z]_t &= \frac{[cz^*]_0}{k_f + k_r} \left\{ k_f [1 - e^{-k_s t}] + \frac{k_s k_f}{k_f + k_r + k_s} [1 - e^{-(k_f + k_r + k_s)t}] \right\} \end{aligned} \quad (4)$$

As stated earlier, for most peptide ECD experiments, when the excite/detect event happens, nearly all fragment ion pairs have already fallen apart. In other words,  $t$  in the above solution at the time of detection can be approximated as infinity when considering the product branching ratio, giving:

$$\frac{[z^*]}{[z]} = \frac{k_r + k_s}{k_f} \quad (5)$$

In the extreme case where the separation of product ions is much slower than the intracomplex hydrogen transfer, i.e.,  $k_s \ll k_r$ , the ratio is governed primarily by thermodynamics, giving the equilibrium constant between the  $c/z\cdot$  and  $c\cdot/z$  ion pairs. In the other extreme case where the separation of product ions is much faster than the intracomplex hydrogen transfer, i.e.,  $k_s \gg k_r$ , the ratio is kinetically controlled, with the eq 5 reduced to the familiar form of  $[z\cdot]/[z] = k_s/k_f$ , giving the branching ratio of a parallel or competitive reactions.

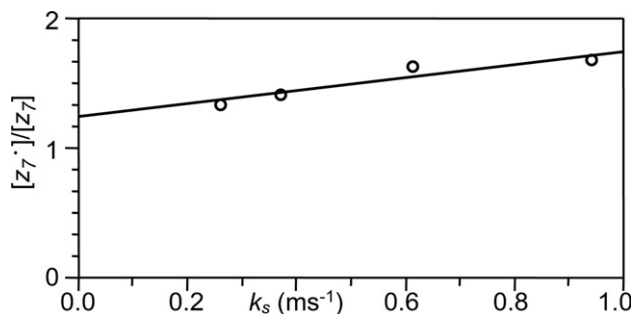


Figure 6. Linear fit of the ratio of the  $z_7\cdot$  and  $z_7$  abundances as a function of the ion separation rate constant as calculated from the DR-ECD experiments.

Equation 5 can be rearranged as:

$$\frac{[z^*]}{[z]} = \frac{k_r}{k_f} + \frac{1}{k_f}k_s \quad (6)$$

With different delays between IR and ECD events, a set of  $[z^*]/[z]$  values can be obtained, with the corresponding  $k_s$  calculated from the DR-ECD experiment, and fit into a straight line. Figure 6 shows one such plot for fibrinopeptide B, using the ratio of  $[z^*]/[z]$  and the  $k_s$  values from Figure 3. The linear regression fit gives a  $k_f$  of  $2.0 \text{ ms}^{-1}$  and a  $k_r$  of  $2.4 \text{ ms}^{-1}$ . The quality of the fit is only moderate, with an  $\sim 0.94$  correlation coefficient, likely because of the assumption that  $k_f$  and  $k_r$  are independent of the folding state. Nevertheless, the obtained hydrogen transfer rates are nearly an order of magnitude higher than the rate of product ion pair separation under normal ECD conditions. It is thus of no surprise that  $c\cdot$  and  $z$  type ions are commonly observed in peptide ion ECD, as the initially formed  $c/z$ -ion pairs have plenty of time to undergo intracomplex hydrogen transfer before they separate to produce individual fragment ions. Despite this fast intracomplex hydrogen transfer rate,  $c\cdot$  and  $z$  type ions are rarely observed in protein ion ECD experiments. Coulombic repulsion between positively charged  $c$  and  $z\cdot$  counterparts, which are not present in the ECD products of doubly charged tryptic peptide ions, may lead to faster product ion separation in protein ion ECD, contributing to this lack of H-transfer products. However, such is not always the case as demonstrated in the DR-ECD experiment of bovine ubiquitin, where many product ions displayed significant abundance drop upon resonant ejection of the charge reduced molecular ion, indicating millisecond lifetimes (at least) of the fragment ion complexes [54]. Presumably, the much more extensive noncovalent interactions in protein ions outweigh the coulombic repulsion in determining the lifetime of intermediates. Most likely, in protein ion ECD, H-transfer still occurs extensively before product ion separation, but somehow preferentially within the  $z\cdot$  fragment itself leading to radical stabilization, possibly due to the tertiary structure of the gas-phase protein ion.

The percentage of the unfolded peptide ions at any given time delay  $t$  is very different for Figure 4 and Figure 5, because of different definitions of an unfolded peptide in two methods. For the DR-ECD approach, fragment ion pair complexes from an unfolded peptide cannot have a lifetime longer than the ejection time, while for the H-transfer method, they cannot undergo any (observable) intracomplex H-transfer before they break apart to produce  $c$  and  $z\cdot$  ions. Since  $t_{1/2}$  of H-transfer is much shorter than the ejection time applied in DR-ECD studies, a significant amount of ion complexes from “unfolded” peptide ions in the DR-ECD approach may still live long enough to generate H-transfer products, and are therefore considered “folded” peptides in the H-transfer method. Regardless, despite different ways to probe the folding state of the

peptide ions, these two methods give similar refolding time constants. When there are abundant  $c\cdot$  or  $z$  type ions, the H-transfer approach is convenient, and has the potential of probing folded state that produces fragment ion pairs shorter lived than that can be probed by the IR-DR-ECD approach, as the typical half-life for H-transfer is only a fraction of the ejection time commonly applied. However, not all peptide ions produce appreciable amounts of  $c\cdot$  or  $z$  type ions, and when this is the result of intrafragment radical stabilization rather than ultrafast fragment ion pair separation, the IR-DR-ECD method should provide an excellent way to study the folding kinetics.

## Conclusions

The effect of IR irradiation on the ECD fragmentation pattern of peptide ions was investigated using two model peptides, Substance P and fibrinopeptide B. The increased internal energy of the precursor ions often led to amplified secondary fragmentation in IR-ECD. Ion activation was accompanied by increased conformational heterogeneity and weakened noncovalent intramolecular interactions. Improved sequence coverage was observed in both peptide ions, likely the result of the conformational change, rather than faster fragment ion separation, as suggested by the lack of sequence coverage improvement when IR irradiation was introduced after the ECD event. Weakening of noncovalent interactions did not lead to appreciable enhancement of fragment ion yield because even at ambient temperature, fragment ion pair separation from small peptide ECD was nearly complete before ion excitation and detection, making IR-ECD unsuitable for probing gas-phase peptide ion folding states. However, IR unfolding of peptide ions did lead to increased  $c/c\cdot$  and decreased  $z/z\cdot$  ratios, which can be utilized to study the peptide refolding process. The refolding rate constant for fibrinopeptide B was measured to be  $\sim 1.5 \text{ s}^{-1}$ , much faster than that of protein ions. Linear regression fit based on a simplified kinetic model of intracomplex hydrogen transfer gave the H-transfer rate constant of  $\sim 2 \text{ ms}^{-1}$ , about an order of magnitude faster than the separation rate of the long-lived  $c/z$  ion pair, explaining the ubiquitous presence of  $c\cdot$  and  $z$  type ions in peptide ion ECD spectra. Alternatively, the folding kinetics of peptide ions can be studied by the IR-DR-ECD method. Rapid resonant ejection of the charge reduced species during ECD can lead to difference in fragment ion yields for folded and unfolded peptide ions, which were indistinguishable under normal ECD conditions, thus making it a suitable probe for folding studies. This approach gave a very similar folding time as that obtained by monitoring the extent of hydrogen transfer, and can be especially useful when no appreciable  $c\cdot$  and  $z$  type ions are present in the ECD spectrum.

## Acknowledgments

The authors gratefully acknowledge the financial support from the National Institutes of Health (grants NIH/NICRR P41RR10888, NIH/NHLBI N01HV28178, and NIH/NIGMS R01GM078293), MDS SCIEX, and the ACS Petroleum Research Fund. They thank Dr. Chunxiang Yao and Xiaojuan Li for help with experiments.

## References

- Gething, M. J.; Sambrook, J. Protein Folding in the Cell. *Nature* **1992**, *355*, 33–45.
- Dobson, C. M. Protein Folding and Misfolding. *Nature* **2003**, *426*, 884–890.
- Fenn, J. B.; Mann, M.; Meng, C. K.; Wong, S. F.; Whitehouse, C. M. Electrospray Ionization for Mass Spectrometry of Large Biomolecules. *Science* **1989**, *246*, 64–71.
- Chowdhury, S. K.; Katta, V.; Chait, B. T. Differences in Charge States of Electrosprayed Native and Denatured Proteins. *J. Am. Chem. Soc.* **1990**, *112*, 9012.
- Loo, J. A. Electrospray Ionization Mass Spectrometry: A Technology for Studying Noncovalent Macromolecular Complexes. *Int. J. Mass Spectrom.* **2000**, *200*, 175–186.
- Winger, B. E.; Light-Wahl, K. J.; Rockwood, A. L.; Smith, R. D. Probing Qualitative Conformation Differences of Multiply Protonated Gas-Phase Proteins via H/D Isotopic Exchange with D<sub>2</sub>O. *J. Am. Chem. Soc.* **1992**, *114*, 5897–5898.
- Suckau, D.; Shi, Y.; Beu, S. C.; Senko, M. W.; Quinn, J. P.; Wampler, F. M., III; McLafferty, F. W. Coexisting Stable Conformations of Gaseous Protein Ions. *Proc. Natl. Acad. Sci. U.S.A.* **1993**, *90*, 780.
- Freitas, M. A.; Hendrickson, C. L.; Emmett, M. R.; Marshall, A. G. Gas-Phase Bovine Ubiquitin Cation Conformations Resolved by Gas-Phase Hydrogen/Deuterium Exchange Rate and Extent. *Int. J. Mass Spectrom.* **1999**, *187*, 565–575.
- Wyttenbach, T.; Bowers, M. T. Gas Phase Conformations of Biological Molecules: The Hydrogen/Deuterium Exchange Mechanism. *J. Am. Soc. Mass Spectrom.* **1999**, *10*, 9–14.
- Robinson, E. W.; Williams, E. R. Multidimensional Separations of Ubiquitin Conformers in the Gas Phase: Relating Ion Cross Sections to H/D Exchange Measurements. *J. Am. Soc. Mass Spectrom.* **2005**, *16*, 1427–1437.
- Clemmer, D. E.; Hudgins, R. R.; Jarrold, M. F. Naked Protein Conformations—Cytochrome-*c* in the Gas-Phase. *J. Am. Chem. Soc.* **1995**, *117*, 10141–10142.
- Jarrold, M. F. Peptides and Proteins in the Vapor Phase. *Annu. Rev. Phys. Chem.* **2000**, *51*, 179–207.
- Badman, E. R.; Myung, S.; Clemmer, D. E. Evidence for Unfolding and Refolding of Gas-Phase Cytochrome *c* Ions in a Paul trap. *J. Am. Soc. Mass Spectrom.* **2005**, *16*, 1493–1497.
- Purves, R. W.; Barnett, D. A.; Guevremont, R. Separation of Protein Conformers Using Electrospray-High Field Asymmetric Waveform Ion Mobility Spectrometry-Mass Spectrometry. *Int. J. Mass Spectrom.* **2000**, *197*, 163–177.
- Robinson, E. W.; Leib, R. D.; Williams, E. R. The Role of Conformation on Electron Capture Dissociation of Ubiquitin. *J. Am. Soc. Mass Spectrom.* **2006**, *17*, 1469–1479.
- Oh, H.; Breuker, K.; Sze, S. K.; Ge, Y.; Carpenter, B. K.; McLafferty, F. W. Secondary and Tertiary Structures of Gaseous Protein Ions Characterized by Electron Capture Dissociation Mass Spectrometry and Photo-fragment Spectroscopy. *Proc. Natl. Acad. Sci. U.S.A.* **2002**, *99*, 15863–15868.
- Oh, H. B.; Lin, C.; Hwang, H. Y.; Zhai, H. L.; Breuker, K.; Zabrowskov, V.; Carpenter, B. K.; McLafferty, F. W. Infrared Photodissociation Spectroscopy of Electrosprayed Ions in a Fourier Transform Mass Spectrometer. *J. Am. Chem. Soc.* **2005**, *127*, 4076–4083.
- Valle, J. J.; Eyley, J. R.; Oomens, J.; Moore, D. T.; van der Meer, A. F. G.; von Helden, G.; Meijer, G.; Hendrickson, C. L.; Marshall, A. G.; Blakney, G. T. Free Electron Laser-Fourier Transform Ion Cyclotron Resonance Mass Spectrometry Facility for Obtaining Infrared Multiphoton Dissociation Spectra of Gaseous Ions. *Rev. Sci. Instrum.* **2005**, *76*.
- Oomens, J.; Polfer, N.; Moore, D. T.; van der Meer, L.; Marshall, A. G.; Eyley, J. R.; Meijer, G.; von Helden, G. Charge-State Resolved Mid-Infrared Spectroscopy of a Gas-Phase Protein. *Phys. Chem., Chem. Phys.* **2005**, *7*, 1345–1348.
- Lin, C.; Infusini, G.; Oh, H.; Hwang, H. Y.; Breuker, K.; Kong, X.; Carpenter, B. K.; McLafferty, F. W. Infrared Photodissociation Spectroscopy of Gaseous Protein Ions. Techniques and Unusual Hydrogen Bonding; unpublished.
- Zubarev, R. A.; Kelleher, N. L.; McLafferty, F. W. Electron Capture Dissociation of Multiply Charged Protein Cations. A Nonergodic Process. *J. Am. Chem. Soc.* **1998**, *120*, 3265–3266.
- Leymarie, N.; Costello, C. E.; O'Connor, P. B. Electron Capture Dissociation Initiates a Free Radical Reaction Cascade. *J. Am. Chem. Soc.* **2003**, *125*, 8949–8958.
- Zubarev, R. A.; Horn, D. M.; Fridriksson, E. K.; Kelleher, N. L.; Kruger, N. A.; Lewis, M. A.; Carpenter, B. K.; McLafferty, F. W. Electron Capture Dissociation for Structural Characterization of Multiply Charged Protein Cations. *Anal. Chem.* **2000**, *72*, 563–573.
- Horn, D. M.; Breuker, K.; Frank, A. J.; McLafferty, F. W. Kinetic Intermediates in the Folding of Gaseous Protein Ions Characterized by Electron Capture Dissociation Mass Spectrometry. *J. Am. Chem. Soc.* **2001**, *123*, 9792–9799.
- Breuker, K.; Oh, H. B.; Horn, D. M.; Cerda, B. A.; McLafferty, F. W. Detailed Unfolding and Folding of Gaseous Ubiquitin Ions Characterized by Electron Capture Dissociation. *J. Am. Chem. Soc.* **2002**, *124*, 6407–6420.
- Breuker, K.; Oh, H. B.; Lin, C.; Carpenter, B. K.; McLafferty, F. W. Nonergodic and Conformational Control of the Electron Capture Dissociation of Protein Cations. *Proc. Natl. Acad. Sci. U.S.A.* **2004**, *101*, 14011–14016.
- Comisarow, M. B.; Marshall, A. G. Fourier Transform Ion Cyclotron Resonance Spectroscopy. *Chem. Phys. Lett.* **1974**, *25*, 282–283.
- Marshall, A. G.; Hendrickson, C. L.; Jackson, G. S. Fourier Transform Ion Cyclotron Resonance Mass Spectrometry: A primer. *Mass Spectrom. Rev.* **1998**, *17*, 1–35.
- Horn, D. M.; Zubarev, R. A.; McLafferty, F. W. Automated de Novo Sequencing of Proteins by Tandem High-Resolution Mass Spectrometry. *Proc. Natl. Acad. Sci. U.S.A.* **2000**, *97*, 10313–10317.
- Ge, Y.; Lawhorn, B. G.; ElNaggar, M.; Strauss, E.; Park, J. H.; Begley, T. P.; McLafferty, F. W. Top Down Characterization of Larger Proteins (45 kDa) by Electron Capture Dissociation Mass Spectrometry. *J. Am. Chem. Soc.* **2002**, *124*, 672–678.
- Zubarev, R. A. Electron-Capture Dissociation Tandem Mass Spectrometry. *Curr. Opin. Biotechnol.* **2004**, *15*, 12–16.
- Cooper, H. J.; Hakansson, K.; Marshall, A. G. The Role of Electron Capture Dissociation in Biomolecular Analysis. *Mass Spectrom. Rev.* **2005**, *24*, 201–222.
- Savitski, M. M.; Nielsen, M. L.; Kjeldsen, F.; Zubarev, R. A. Proteomics-Grade de Novo Sequencing Approach. *J. Proteome Res.* **2005**, *4*, 2348–2354.
- Sze, S. K.; Ge, Y.; Oh, H.; McLafferty, F. W. Top-Down Mass Spectrometry of a 29-kDa Protein for Characterization of Any Post-translational Modification to Within One Residue. *Proc. Natl. Acad. Sci. U.S.A.* **2002**, *99*, 1774–1779.
- Pesavento, J. J.; Kim, Y.-B.; Taylor, G. K.; Kelleher, N. L. Shotgun Annotation of Histone Modifications: A New Approach for Streamlined Characterization of Proteins by Top Down Mass Spectrometry. *J. Am. Chem. Soc.* **2004**, *126*, 3386–3387.
- Meng, F.; Forbes, A. J.; Miller, L. M.; Kelleher, N. L. Detection and Localization of Protein Modifications by High Resolution Tandem Mass Spectrometry. *Mass Spectrom. Rev.* **2005**, *24*, 126–134.
- Savitski, M. M.; Nielsen, M. L.; Zubarev, R. A. ModifiComb, a new Proteomic Tool for Mapping Substoichiometric Post-translational Modifications, Finding Novel Types of Modifications, and Fingerprinting Complex Protein Mixtures. *Mol. Cell. Proteom.* **2006**, *5*, 935–948.
- Zhao, C.; Sethuraman, M.; Clavreul, N.; Kaur, P.; Cohen, R. A.; O'Connor, P. B. Detailed Map of Oxidative Post-translational Modifications of Human P21Ras Using Fourier Transform Mass Spectrometry. *Anal. Chem.* **2006**, *78*, 5134–5142.
- Patriksson, A.; Adams, C.; Kjeldsen, F.; Raber, J.; van der Spoel, D.; Zubarev, R. A. Prediction of NC(α) Bond Cleavage Frequencies in Electron Capture Dissociation of Trp-Cage Dications by Force-Field Molecular Dynamics Simulations. *Int. J. Mass Spectrom.* **2006**, *248*, 124–135.
- Tsybin, Y. O.; He, H.; Hamidane, H. B.; Emmett, M. R.; Hendrickson, C. L.; Tsybin, O. Y.; Marshall, A. G. Electron Capture/Transfer Dissociation Product Ion Abundances: Correlation with Amino Acid Hydrophobicity and Application in Peptide and Protein Structural Analysis. *Proceedings of the 54th ASMS Conference on Mass Spectrometry and Allied Topics*; Indianapolis, IN, June 2007; DVD-ROM.
- Horn, D. M.; Ge, Y.; McLafferty, F. W. Activated Ion Electron Capture Dissociation for Mass Spectral Sequencing of Larger (42 kDa) Proteins. *Anal. Chem.* **2000**, *72*, 4778–4784.
- Hakansson, K.; Chalmers, M. J.; Quinn, J. P.; McFarland, M. A.; Hendrickson, C. L.; Marshall, A. G. Combined Electron Capture and Infrared Multiphoton Dissociation for Multistage MS/MS in a Fourier Transform Ion Cyclotron Resonance Mass Spectrometer. *Anal. Chem.* **2003**, *75*, 3256–3262.
- Sze, S. K.; Ge, Y.; Oh, H. B.; McLafferty, F. W. Plasma Electron Capture Characterization of Large Dissociation for the Proteins by Top Down Mass Spectrometry. *Anal. Chem.* **2003**, *75*, 1599–1603.
- Tsybin, Y. O.; Witt, M.; Baykut, G.; Kjeldsen, F.; Hakansson, P. Combined Infrared Multiphoton Dissociation and Electron Capture Dissociation with a Hollow Electron Beam in Fourier Transform Ion Cyclotron Resonance Mass Spectrometry. *Rapid Commun. Mass Spectrom.* **2003**, *17*, 1759–1768.
- Oh, H. B.; McLafferty, F. W. A Variety of Activation Methods Employed in “Activated-Ion” Electron Capture Dissociation Mass Spectrometry: A Test Against Bovine Ubiquitin 7<sup>+</sup>-ions. *Bull. Korean Chem. Soc.* **2006**, *27*, 389–394.
- Coumoyer, J. C.; Lin, C.; O'Connor, P. B. Using H(dot) Transfer from Electron Capture Dissociation Fragmentation Spectra to Probe the Gas-Phase Structure of Peptides, unpublished.
- Gauthier, J. W.; Trautman, T. R.; Jacobson, D. B. Sustained Off-Resonance Irradiation for Collision-Activated Dissociation Involving Fourier-Transform Mass Spectrometry-Collision-Activated Dissocia-

- tion Technique that Emulates Infrared Multiphoton Dissociation. *Anal. Chim. Acta* **1991**, *246*, 211–225
48. Mirgorodskaya, E.; O'Connor, P. B.; Costello, C. E. A General Method for Precalculation of Parameters for Sustained Off Resonance Irradiation/Collision-Induced Dissociation. *J. Am. Soc. Mass Spectrom.* **2002**, *13*, 318–324.
49. Dunbar, R. C.; McMahon, T. B. Activation of Unimolecular Reactions by Ambient Blackbody Radiation. *Science* **1998**, *279*, 194–197.
50. Price, W. D.; Schnier, P. D.; Williams, E. R. Tandem Mass Spectrometry of Large Biomolecule Ions by Blackbody Infrared Radiative Dissociation. *Anal. Chem.* **1996**, *68*, 859–866.
51. O'Connor, P. B.; Lin, C.; Cournoyer, J. J.; Pittman, J. L.; Belyayev, M.; Budnik, B. A. Long-Lived Electron Capture Dissociation Product Ions Experience Radical Migration via Hydrogen Abstraction. *J. Am. Soc. Mass Spectrom.* **2006**, *17*, 576–585.
52. Savitski, M. M.; Kjeldsen, F.; Nielsen, M. L.; Zubarev, R. A. Hydrogen Rearrangement to and from Radical z Fragments in Electron Capture Dissociation of Peptides. *J. Am. Soc. Mass Spectrom.* **2007**, *18*, 113–120.
53. Tsybin, Y. O.; He, H.; Emmett, M. R.; Hendrickson, C. L.; Marshall, A. G. Ion Activation in Electron Capture Dissociation to Distinguish Between N-Terminal and C-Terminal Product Ions. *Anal. Chem.* **2007**, *79*, 7596–7602.
54. Lin, C.; O'Connor, P. B.; Cournoyer, J. J. Use of a Double Resonance Electron Capture Dissociation Experiment to Probe Fragment Intermediate Lifetimes. *J. Am. Soc. Mass Spectrom.* **2006**, *17*, 1605–1615.
55. O'Connor, P. B.; Pittman, J. L.; Thomson, B. A.; Budnik, B. A.; Cournoyer, J. C.; Jebanathirajah, J.; Lin, C.; Moyer, S.; Zhao, C. A New Hybrid Electrospray Fourier Transform Mass Spectrometer: Design and Performance Characteristics. *Rapid Commun. Mass Spectrom.* **2006**, *20*, 259–266.
56. Jebanathirajah, J. A.; Pittman, J. L.; Thomson, B. A.; Budnik, B. A.; Kaur, P.; Rape, M.; Kirschner, M.; Costello, C. E.; O'Connor, P. B. Characterization of a New qQQ-FTICR Mass Spectrometer for Post-translational Modification Analysis and Top-Down Tandem Mass Spectrometry of Whole Proteins. *J. Am. Soc. Mass Spectrom.* **2005**, *16*, 1985–1999.
57. Mihalca, R.; Kleinnijenhuis, A. J.; McDonnell, L. A.; Heck, A. J. R.; Heeren, R. M. A. Electron Capture Dissociation at Low Temperatures Reveals Selective Dissociations. *J. Am. Soc. Mass Spectrom.* **2004**, *15*, 1869–1873.
58. Gill, A. C.; Jennings, K. R.; Wyttenbach, T.; Bowers, M. T. Conformations of Biopolymers in the Gas Phase: A New Mass Spectrometric Method. *Int. J. Mass Spectrom.* **2000**, *196*, 685–697.
59. Liu, H. C.; Hakansson, K. Divalent Metal Ion-Peptide Interactions Probed by Electron Capture Dissociation of Trications. *J. Am. Soc. Mass Spectrom.* **2006**, *17*, 1731–1741.
60. Cooper, H. J.; Hudgins, R. R.; Hakansson, K.; Marshall, A. G. Secondary Fragmentation of Linear Peptides in Electron Capture Dissociation. *Int. J. Mass Spectrom.* **2003**, *228*, 723–728.
61. Zubarev, R. A. Reactions of Polypeptide Ions with Electrons in the Gas Phase. *Mass Spectrom. Rev.* **2003**, *22*, 57–77.
62. Turecek, F. N–C- $\alpha$  Bond Dissociation Energies and Kinetics in Amide and Peptide Radicals. Is the Dissociation a Nonergodic Process? *J. Am. Chem. Soc.* **2003**, *125*, 5954–5963.
63. Yao, C. X.; Syrstad, E. A.; Turecek, F. Electron Transfer to Protonated  $\beta$ -Alanine N-Methylamide in the Gas Phase: An Experimental and Computational Study of Dissociation Energetics and Mechanisms. *J. Phys. Chem. A* **2007**, *111*, 4167–4180.
64. Kjeldsen, F.; Haselmann, K. F.; Budnik, B. A.; Jensen, F.; Zubarev, R. A. Dissociative Capture of Hot (3–13 eV) Electrons by Polypeptide Polycations: An Efficient Process Accompanied by Secondary Fragmentation. *Chem. Phys. Lett.* **2002**, *356*, 201–206.
65. Kjeldsen, F.; Zubarev, R. Secondary Losses Via  $\gamma$ -Lactam Formation in Hot Electron Capture Dissociation: A Missing Link to Complete de Novo Sequencing of Proteins? *J. Am. Chem. Soc.* **2003**, *125*, 6628–6629.
66. Belyayev, M. A.; Cournoyer, J. J.; Lin, C.; O'Connor, P. B. The Effect of Radical Trap Moieties on Electron Capture Dissociation Spectra of Substance P. *J. Am. Soc. Mass Spectrom.* **2006**, *17*, 1428–1436.
67. Hayakawa, S.; Hashimoto, M.; Matsubara, H.; Turecek, F. Dissecting the Proline Effect: Dissociations of Proline Radicals Formed by Electron Transfer to Protonated pro-gly and gly-pro Dipeptides in the Gas Phase. *J. Am. Chem. Soc.* **2007**, *129*, 7936–7949.
68. Jones, J. W.; Sasaki, T.; Goodlett, D. R.; Turecek, F. Electron Capture in Spin-Trap Capped Peptides. An Experimental Example of Ergodic Dissociation in Peptide Cation-Radicals. *J. Am. Soc. Mass Spectrom.* **2007**, *18*, 432–444.